CHAPTER EIGHTEEN

Gravimetric biosensors

Khasim Cali[a], Elena Tuccori[b], Krishna C. Persaud[a,*]
[a]Department of Instrumentation and Analytical Science, The University of Manchester, Manchester, United Kingdom
[b]Pall Corporation, Portsmouth, United Kingdom
*Corresponding author: e-mail address: krishna.persaud@manchester.ac.uk

Contents

Methods in Enzymology, Volume 642
ISSN 0076-6879
https://doi.org/10.1016/bs.mie.2020.05.010

Abstract

Gravimetric transducers produce a signal based on a change in mass. These transducers can be used to construct gas sensors or biosensors using odorant binding proteins (OBPs) as recognition elements for small volatile organic compounds. The methods described in this chapter are based on the immobilization of the OBPs onto functionalized (activated) self-assembled monolayer (SAMs) on gold and on nanocrystalline diamond surfaces. Depending on the surface immobilization methods used to fabricate the biosensor, recombinant proteins can be engineered to express six histidine tags either on the N-terminal or C-terminal of the proteins and these can also be used to facilitate protein immobilization. These methods are used to produce functional sensors based on quartz crystal microbalances or surface acoustic wave devices and are also applicable to other types of gravimetric transducers.

Abbreviations

CMUT	capacitive micromachined ultra-sonic transducer
DCM	dichloromethane
ddH_2O	double distilled water
DMF	dimethylformamide
EDC	1-ethyl-3-[3-dimethylaminopropyl] carbodiimide hydrochloride
FBAR	film bulk acoustic resonator
LB	Langmuir-Blodgett
LIFT	laser induced forward transfer
MEMS	micro-electromechanical system
MUP	major urinary protein
NHS	N-hydroxysuccinimide
NTA	nitrilotriacetic acid, Nα, Nα-Bis-(carboxy-methyl)-L-lysine hydrate
OBP	odorant binding protein
PFA	perfluoroalkoxy
PTFE	polytetrafluoroethylene
QCM	quartz crystal microbalance
Q-Factor	quality factor
SAM	self-assembled monolayer
SAW	surface acoustic wave
SVP	saturated vapor pressure
TA	thioctic acid

1. Introduction

A gravimetric transducer produces a signal based on a change in mass (Fanget et al., 2011). For gas sensors or biosensors, a sensitive coating is utilized. Mass loading of the transducer is related to parameters describing

the efficiency of analyte adsorption onto the sensitive coating. The partition coefficient K describes the adsorbing properties of the layer at equilibrium. K depends on chemical, vapor solubility properties, polarizability, dipolarity, hydrogen bond acidity, hydrogen bond basicity interactions, between analyte molecules and the sorbent layer. This chapter focusses on the use of gravimetric transducers to construct gas sensors or biosensors using odorant binding proteins (OBPs) as the sorbent elements for different classes of chemical species. Incorporating the sensing components of biological olfaction systems can increase the selectivity and sensitivity of the resulting sensors and has promise to overcome the limitations of materials normally used in sorptive based gas sensors or biosensors. Persaud and Tuccori demonstrated that OBPs can be successfully immobilized on quartz crystal microbalances to produce viable gas sensors capable of sensing pheromones (Persaud & Tuccori, 2014). Subsequently it was demonstrated that OBPs and the closely related family of major urinary proteins (MUPs) could be immobilized on microcantilever devices or surface acoustic wave transducers to produce robust and sensitive gas sensor arrays (Cali, Scorsone, & Persaud, 2019; Manai et al., 2014; Scorsone et al., 2016).

The methods described in this chapter are based on the immobilization of the OBPs onto functionalized (activated) self-assembled monolayer (SAMs) on gold (for quartz crystal microbalance (QCM) biosensors) and on diamond (for surface acoustic wave (SAW) biosensors). Depending on the surface immobilization methods used to fabricate the biosensor, recombinant proteins can be engineered to express six histidine tags either on the N-terminal or C-terminal of the proteins and these can also be used to facilitate protein immobilization.

1.1 The piezoelectric effect

The discovery of the piezoelectric effect by Jaques and Pierre Curie in 1880 (Curie & Curie, 1880) opened a new era of research relating mechanical states and electrical states in crystals. They demonstrated that when crystals such as Quartz or Rochelle salt (sodium potassium tartrate tetrahydrate) were compressed, an electrical potential could be measured between the faces of the crystals. Lippmann predicted the converse effect should also occur (Lippmann, 1881) which was also verified by the Curie brothers. In 1917, Langevin suggested the design for the first piezoelectric transducer based on these studies, employing quartz plates to serve as emitters and receivers of high-frequency waves under water that led to the development of sonar, Rutherford also being instrumental in employing piezoelectric devices as hydrophones (Katzir, 2012).

The nature of piezoelectricity is linked to the number of electric dipoles present in the material. A dipole is a vector having a direction and a value dependent on the other electrical charges in the vicinity. These dipoles tend to have the same direction when next to each other forming regions called Weiss domains (Weiss, 1906) that are generally randomly oriented. With some materials these domains can be aligned by poling which is a process by which a strong electric field is applied across the material. The reason why piezoelectric material creates a voltage is because when a mechanical stress is applied, the crystalline structure is disturbed changing the direction of the polarization of the electric dipoles. Depending on the nature of the dipole this change in the polarization might either be caused by a reconfiguration of the ions within the crystalline structure or by a reorientation of molecular groups. The resulting change in dimensions from an applied stress can shift the centers of mass for the positive and negative ions thus producing a dipole throughout the material (Fig. 1).

The dipoles inside the material cancel each other out, but on the surface of the material this cannot happen, producing a polarity on the surface due to the surface charge density. If electrodes are connected to the faces of a thin slab of this material and these are connected to a current measurement device, a current can be measured through the external circuit when stress is applied to the crystal. Releasing the stress causes a transient current flow in the opposite direction. If the converse effect is used and an alternating potential difference applied, mechanical oscillations occur within the crystal lattice. Stable oscillations occur at the natural resonant frequency of the crystal and at that frequency the crystal presents a low impedance to the exciting voltage. If the crystal is incorporated into the feedback loop of an oscillating circuit, it becomes the frequency determining element of the circuit, as its Q (quality factor—defined as the ratio of the energy stored in the oscillating resonator to the energy dissipated per cycle by damping processes) is very high, typically several thousand. Pioneering researchers such as Cady (Cady, 1921, 1946), Pierce (Pierce, 1923) and others designed crystal controlled oscillators with high stability for use as tuning devices and crystal filters for communication lines and radio that are now embedded in a multitude of modern electronic devices. A quartz crystal has a hexagonal prism structure as shown in Fig. 1C. The z-axis runs along the length of the crystal and is called the optical axis. The x-axis or the electric axis is parallel to a line bisecting the angles between adjacent prism faces. The y-axis, which is also known as the mechanical axis, is at right angles to the face of prism and also to the x-axis. Initially oscillator crystals were cut in the y-z plane with the electric field applied along the x-axis. These crystals were rather unstable and

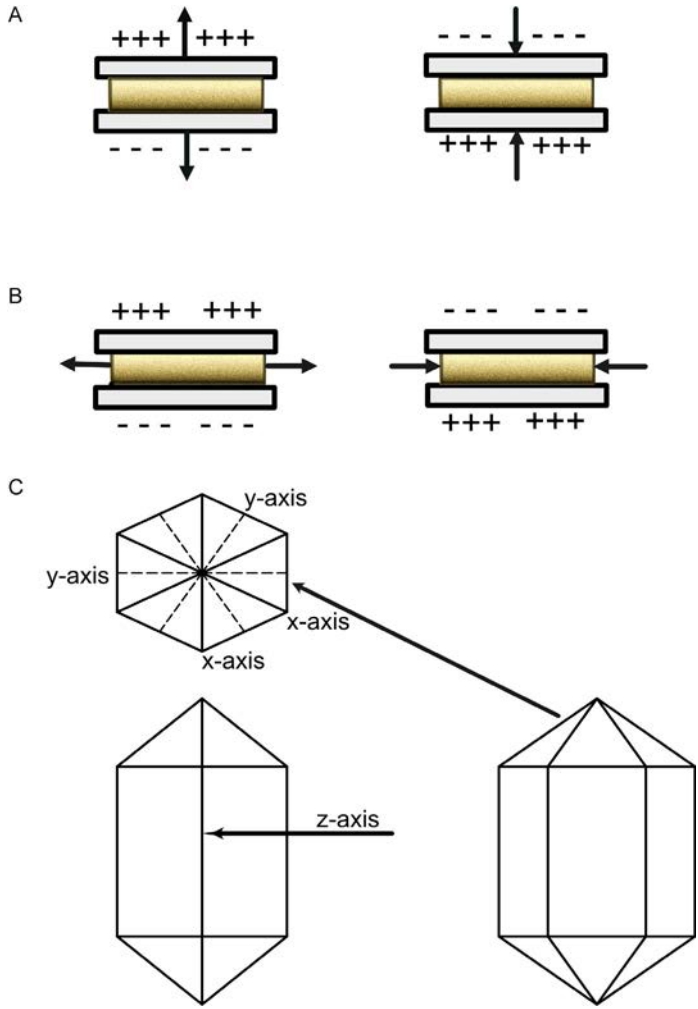

Fig. 1 The piezoelectric effect is illustrated; mechanical tension or compression on a piezoelectric material will induce a current depending type of stress and direction shown by the arrows shown in (A) and (B). When a stress is applied to a piezoelectric material, the dimensions of the material changes. Depending on the direction the stress is applied, the resulting change in dimensions can shift the centers of mass for the positive and negative ions; this produces a dipole throughout the material. The dipoles inside the material cancel each other out, but on the surface of the material the dipoles are not canceled out, producing a polarity between the faces of the material. (C) A quartz crystal has a hexagonal prism structure shown on the right. As shown on the left, the z-axis runs along the length of the crystal and is called the optical axis. The x-axis or the electric axis is parallel to a line bisecting the angles between adjacent prism faces. The y-axis, which is also known as the mechanical axis, shown in dotted lines, is at right angles to the face of prism and also to the x-axis.

could only work at low frequencies. Lack, Willard, and Fair (1930) showed that cutting crystals at various angles changed the temperature coefficients and frequency constants. Experiments with different cuts of crystals yielded two cuts with zero temperature coefficients +35°15′ (AT cut), and −49°00′ (BT cut) and these have been widely adopted since then.

1.2 Quartz crystal microbalances and chemical sensing

In 1959, Sauerbrey established a relationship between mass absorption on the surface of an AT-cut quartz crystal and offset of its frequency in gas phase, which established the foundation for quartz crystal microbalance (QCM) research in the area of chemical sensing (Sauerbrey, 1959). This relationship is summarized in Eq. (1)

$$\Delta f = \frac{-2 {f_0}^2}{A\sqrt{\rho_q \mu_q}} \Delta m, \tag{1}$$

where

Δf = the measured resonant frequency change (Hz)
f_0 = the intrinsic frequency of the quartz crystal (Hz)
A = the piezoelectrically active crystal area (electrodes area, cm^2)
ρ_q = the density of quartz ($2.643\,g/cm^2$)
μ_q = the shear modulus of quartz for the AT-cut crystal ($2.947 \times 10^{11}\,g/cm\,s^2$)
Δm = the elastic mass change (g)

This simplifies to

$$\Delta f = -2.26.10^{-6} \frac{f_0^2}{A} \Delta m \tag{2}$$

King (1972) described a piezoelectric sorption detector and demonstrated its ability to measure extremely small mass changes in an air environment. He also described an approach which should be taken to extend this concept to liquid systems. For quartz crystals coated with various materials the Sauerbrey equation only applies to the elastic subjects such as metallic coatings, metal oxides, and thin adsorbed layers that do not dissipate energy during the oscillation and there may be substantial deviations due to viscoelastic effects of coatings (Vogt, Lin, Wu, & White, 2004).

QCMs have gained widespread use in creating arrays of gas sensors (Di Natale et al., 2008; Muñoz-Aguirre, Nakamoto, & Moriizumi, 2005; Nakamoto, Fukunishi, & Moriizumi, 1990), and have been widely adopted as transducers for "electronic nose" technologies. Fig. 2 shows a picture of

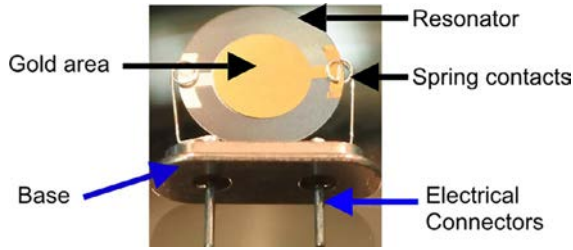

Fig. 2 An AT-cut 20 MHz quartz crystal is shown. The resonator is supported by two spring contacts at the edges. These make electrical and mechanical contact with evaporated gold disks deposited on both sides of the QCM and are connected to the electrical contacts on the crystal base. The crystal sets the base frequency of an oscillator circuit that produces a train of electrical pulses at a frequency set by the resonant frequency of the crystal.

a quartz crystal commonly used as a transducer for gas sensors. It has a resonance frequency of 20 MHz and is 7.95 mm in diameter. On both sides of the crystal is a thin layer of gold (4.9 mm diameter) which is evaporated over a titanium adhesion layer and this is used for immobilization of sorbent materials such as polymers, proteins or other materials. Electrical connections are made via spring contacts that are clamped to the gold connectors on the edges of the quartz resonator.

1.3 Surface acoustic wave transducers

Surface acoustic waves (SAWs) are elastic waves, first described by Rayleigh (1885), that can travel along the surface of a solid piezoelectric—the amplitude decaying with depth into the material proportionally to the wavelength. Interdigitated electrodes were utilized by White and Voltmer to generate an acoustic wave across a piezoelectric material (White & Voltmer, 1965) and this concept was used to develop a host of resonant devices that have become commonly used in filters and tuning elements in the electronic industry (e.g., smartphones). Because the mechanical vibrations are a strong function of their environment, including both their frequency and amplitude, changes in the environment can lead to changes in the SAW itself. This forms the basis for a SAW chemical sensor; target analytes change the SAW environment and changes in the SAW are subsequently detected. The physical structure of such a device is shown in Fig. 3.

The most general mode used for gas sensing used is the Rayleigh wave, in which the SAW propagates at the speed of sound of the crystal and the surface displacement has two components—one normal to the SAW propagation and one parallel (shear) to the substrate—resulting in an elliptical

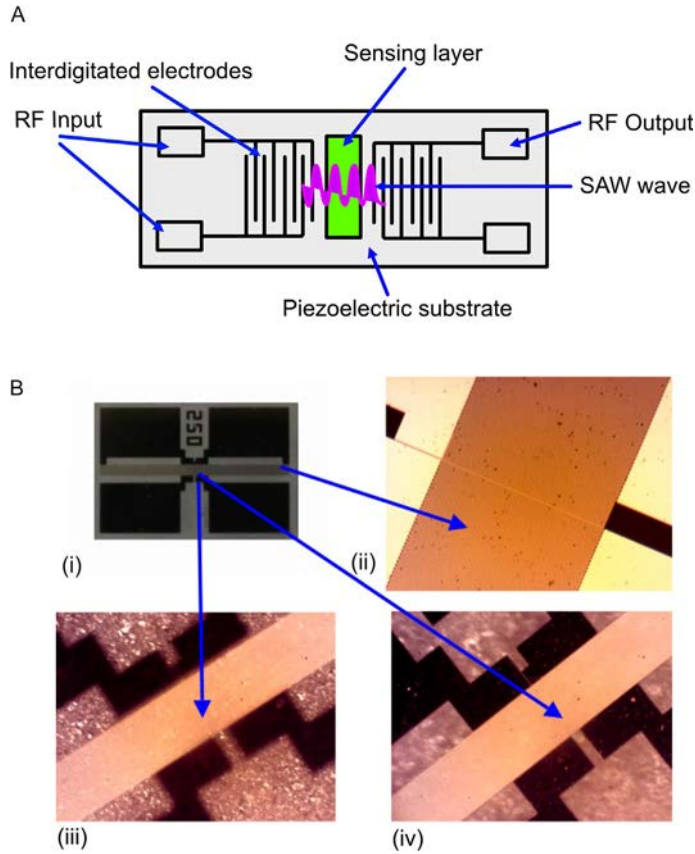

Fig. 3 (A) A schematic of a simple SAW resonator is shown. Two Interdigitated electrode structures (IDT) are deposited on a piezoelectric substrate. This makes up a SAW delay line. One IDT acts as the input or the transmitting IDT which converts radiofrequency (RF) electrical signals to acoustic energy that propagates on the surface of the piezoelectric substrate to the output (IDT) transducer which converts acoustic energy back to an electric signal creating a delay equivalent to the time taken by the surface acoustic wave to travel between the two IDTs. If an adsorbent material is placed between the two IDTs, then adsorption of molecules from the vapor phase on to the material will case a change in the propagation delay of the surface acoustic wave. (B) (i) a SAW transducer manufactured by KIT (Karlsruhe Institute of Technology, Germany)—the band in the center running from left to right constitutes interdigitated electrodes shown in more detail in (ii) the gap between each electrode sets the resonant frequency of the structure. (iii) and (iv) show views of the SAW transducer modified by deposition of nanocrystalline diamond (CEA, France) which allows attachment of OBPs via NTA modified diamond surfaces. *Panel (A) adapted from Voiculescu, I., & Nordin, A. N. (2012). Acoustic wave based MEMS devices for biosensing applications.* Biosensors and Bioelectronics, 33*(1), 1–9.* *https://doi.org/10.1016/j.bios.2011.12.041*.

motion. The Lamb wave (Lamb, 1917) resembles the Rayleigh wave and is typically generated using very thin substrates that are only a few wavelengths thick. These devices can be used also for sensing in liquid media. For sensing in liquids, a thin film called a guiding layer is often applied to the surface of the device to activate a Love wave mode (Love, 1911), which also inhibits radiation of acoustic pressure into the liquid. The interdigitated transducer (IDT) electrode pattern shown in Fig. 2 determines the resonant frequency of the device, where in a typical IDT the electrode spacing is an integer multiple or 1/2, 1/3, or 1/4 of the wavelength $\lambda = 2\pi/k$, with k being the wavenumber. For most devices, the wavelengths are between 0.01 and 1.0 mm. The most basic design is planar where the IDT consists of simple linear electrode "fingers" with equal spacing between them, but many more complex designs have been implemented. SAW devices operate at much higher frequencies than quartz crystals—typical devices are made to resonate at 433 MHz which is within a useful operational waveband for many communications devices.

In general, a SAW chemical sensing system consists of a sensing layer on the SAW substrate that is designed to react or bind with the analytical target, and electrical components designed for read out and recording the sensor output. Any perturbation will alter the delay in propagation of an acoustic wave across the surface of the device. This can be sensed as a phase shift, frequency-shift, or time-delay in the output electrical signal. The sensing layer interacts with the target to cause detectable changes in the characteristics of the acoustic wave, such as the velocity ν or amplitude, which results in a frequency-shift f or phase shift ϕ (Eq. 3).

$$\frac{\Delta\nu}{\nu} = \frac{\Delta f}{f} = -\frac{\Delta\phi}{\phi} \tag{3}$$

The sensing layer is a critical component of sensor design, and a wide variety of sensing layer materials have been explored for both chemical and biological SAW sensors. These include polymers, metal oxides, nanoparticles, or for biological applications proteins such as antibodies. Comprehensive reviews of SAW chemical sensors include Länge, Rapp, and Rapp (2008) and Go, Atashbar, Ramshani, and Chang (2017).

1.4 Film bulk acoustic resonator (FBAR)

The film bulk acoustic resonator is a CMOS compatible sensor based on QCM theory and have a mass sensitivity three orders of magnitude higher than QCM. This is due to the thin films achieved in the structure as

compared to the diced quartz used in QCM. The FBAR membrane structure is well known in MEMS fabrication. A bulk wave propagating inside a piezoelectric thin film is generated by putting the piezoelectric thin film between electrodes and applying a high-frequency signal (Fig. 4). Standing acoustic waves with a defined resonant frequency, f_r, are generated by the rf signal due to the inverse piezoelectric effect. Addition of a mass on the surface of the resonator results in a change in f_r. By tracking changes in f_r, mass changes on the resonators can be detected. Chemical transducers operating at much higher frequencies than SAW devices are now being exploited (Chang et al., 2016; Mastromatteo & Villa, 2013; Tukkiniemi et al., 2009; Zhang, Du, Fang, & Zhao, 2017; Zhang, Luo, Flewitt, Cai, & Zhao, 2018).

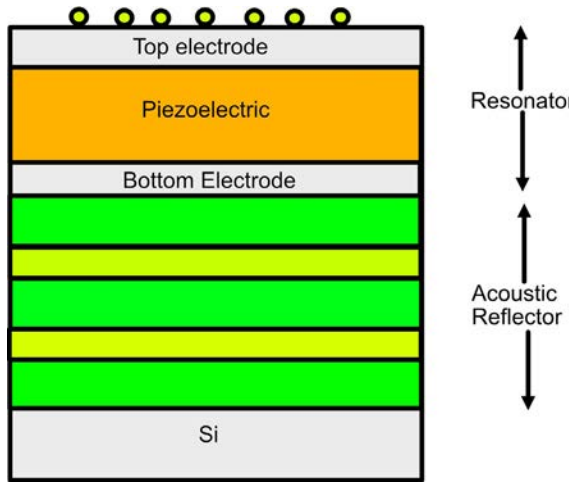

Fig. 4 The structure of a film bulk acoustic resonator (FBAR) is shown. Piezoelectric films fabricated using MEMS technology are thinner, can reach higher frequencies and offers the advantage of monolithic integration with advanced CMOS technology for peripheral readout and signal processing circuitry. FBARs are fabricated from a thin central piezo-electric layer with metal electrodes micropatterned on both sides. The FBAR's Q-factor can be increased by placing it on top of an acoustic mirror. The acoustic mirror is formed using alternating oxide and metallic layers. Acoustic isolation from the substrate is achieved when a Bragg reflector, comprised of layer pairs with contrasting acoustic impedance is placed underneath the FBAR. The exposed electrode at the top of the FBAR can be functionalized to immobilize proteins or other materials to create biosensors. *Adapted from Voiculescu, I., & Nordin, A. N. (2012). Acoustic wave based MEMS devices for biosensing applications.* Biosensors and Bioelectronics, 33*(1), 1–9. https://doi.org/10.1016/j.bios.2011.12.041*.

The wave resonates at a discrete frequency according to the thickness of the thin film. Like SAW the frequency f can be expressed as in Eq. (3) in terms of wavelength λ and acoustic velocity ν:

$$\lambda f_0 = \nu \tag{4}$$

where the wavelength λ is related to the thickness h of the piezoelectric film

$$\lambda = 2h \tag{5}$$

These devices typically operate at around 2 GHz.

1.5 Micro-electromechanical systems (MEMS)

Microcantilevers are small beams which are anchored at one end. Molecular adsorption on a cantilever surface can generate bending as a result of adsorption-induced changes in surface stress. In addition, mass loading due to molecular adsorption results in changes in the resonance frequency of the cantilever (Fig. 5). Chemical or biological selectivity can be achieved

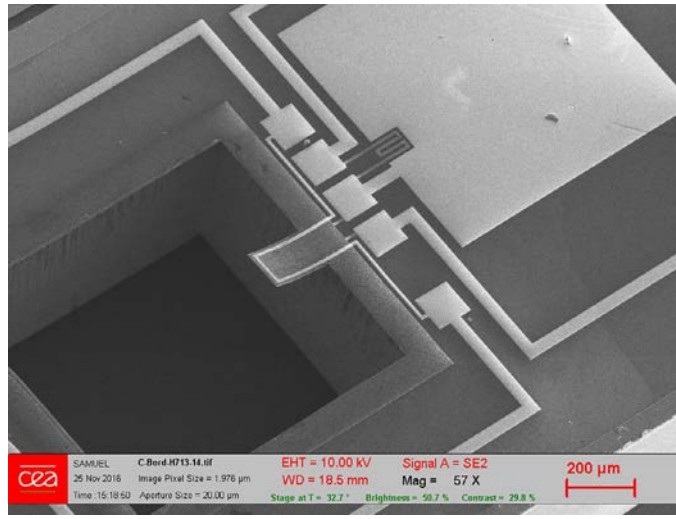

Fig. 5 Photograph of a microcantilever device fabricated by CEA, France. Microcantilever sensors operate by detecting changes in resonance response or deflection caused by mass loading, surface stress variation, or changes in damping conditions. Four resonance response parameters (resonance frequency, amplitude, Q-factor, and deflection) can be detected simultaneously. Surface stress produced as molecules adsorb on a cantilever can be observed as changes in deflections. *Photograph—courtesy of Dr. Emmanuel Scorsone, CEA, France.*

via immobilized sorptive materials on the cantilever surface (Thundat, Oden, & Warmack, 1997). Resonant micro cantilevers with different transduction techniques have been commonly used for gas concentration measurement. Piezoresistive layers are often used to detect the cantilever bending that can be produced by different ways (e.g., electrostatic or magnetic actuation forces). These devices are comprehensively reviewed by Voiculescu and Nordin (2012). Possas-Abreau et al. described the development of diamond and silicon MEMS sensor arrays for vapor detection (Fig. 5) (Possas-Abreu, Ghassemi, et al., 2017).

1.6 Capacitive micromachined ultra-sonic transducer (CMUT)

Capacitive micromachined ultrasonic transducers (CMUT) are membrane micro-electromechanical system (MEMS) devices that use capacitive transduction for mass load detection. They have very small capacitances and it is necessary to connect many CMUT devices into a parallel array. Using the group capacitance, this gives extremely high mass sensitivity afforded by the array of devices and allows for a range of operating frequencies dependent on the thickness of the resonating membrane (Fanget et al., 2011; Nazemi, Joseph, Park, & Emadi, 2019).

2. Protein immobilization

All of the gravimetric transducers described previously are appropriate for producing biosensors or gas sensors based on OBPs. However, care needs to be taken in the immobilization of biomolecules on the transducer surface to ensure optimum sensor performance. The selective immobilization of proteins is a key step in developing useful biosensors, because both protein stability and functionality require special control over protein orientation at the sensitive layers of devices. The techniques used have great effects on the specificity, sensitivity, reproducibility and reversibility of the resulting sensor. Some of the requirements of an immobilization process include: (1) retention of biological activity of biomolecules; (2) achievement of reproducible and stable attachment with the substrate against variations of pH, temperature, ionic strength, chemical nature of the microenvironment; and (3) uniform, dense, and oriented localization of the biomolecules. Bioconjugation, where biomolecules are linked together or to solid supports, is an important aspect of the biological sciences. Noncovalent methods of protein immobilization are widely employed and involve either

passive adsorption on to hydrophobic surfaces or electrostatic interactions with charged surfaces. However, this method often induces conformational changes in the proteins that reduce their binding activity.

For biosensor fabrication it is much more efficient to covalently immobilize the protein via a functional group that is naturally present (Wong, Khan, & Micklefield, 2009). It is possible to couple proteins via exposed amines, e.g., from lysine groups, using an active ester, an aldehyde or epoxides (Fig. 6). The cysteine residue may also be used as the thiol group readily undergoes conjugate addition with α,β-unsaturated carbonyls (e.g., maleimides) to form stable thioether bonds. Similarly carboxylic groups from acidic moieties such as aspartic and glutamic residues, can be immobilized by conversion to their corresponding active esters in situ with a carbodiimide coupling agent such as 1-ethyl-3-(3-dimethylaminopropyl)carbodiimide (EDC) with an auxiliary nucleophile such as N-hydro-succinimide (NHS) (Fig. 7).

Apart from covalent methods it is also possible to use non-covalent but biologically mediated methods of immobilization. The protein can be expressed with a genetically encoded polyhistidine tag (Hochuli, Bannwarth, Dobeli, Gentz, & Stuber, 1988). This tag usually consists of six sequential His residues, and has the ability to chelate transition metals including Cu(II), Co(II), Zn(II), or Ni(II). Thus, a biosensor surface can be modified with a chelating moiety such as nitrilotriacetic acid (NTA) or iminodiacetic acid and is then treated with a solution of the relevant metal salt (commonly nickel) to produce a support containing the metal ions. This metal-activated support is then used for protein immobilization through chelation with the His residues of the tag (Fig. 8).

There are also developments in materials coating the transducer that can improve covalent immobilization of proteins. Coating surface acoustic wave devices or microcantilevers with diamond nanoparticles confers attractive properties for chemical detection. It is a chemically inert material with a high Q-factor producing a stable sensor platform, yet the carbon terminated surface offers wide possibilities for covalent attachment of specific receptors including odorant binding proteins (Chevallier, Scorsone, & Bergonzo, 2009; Manai et al., 2014; Possas-Abreu, Rousseau, et al., 2017).

2.1 Self-assembled monolayers

There has been much research effort dedicated to optimizing the conditions for covalent binding and self-assembled monolayer (SAM) technology has

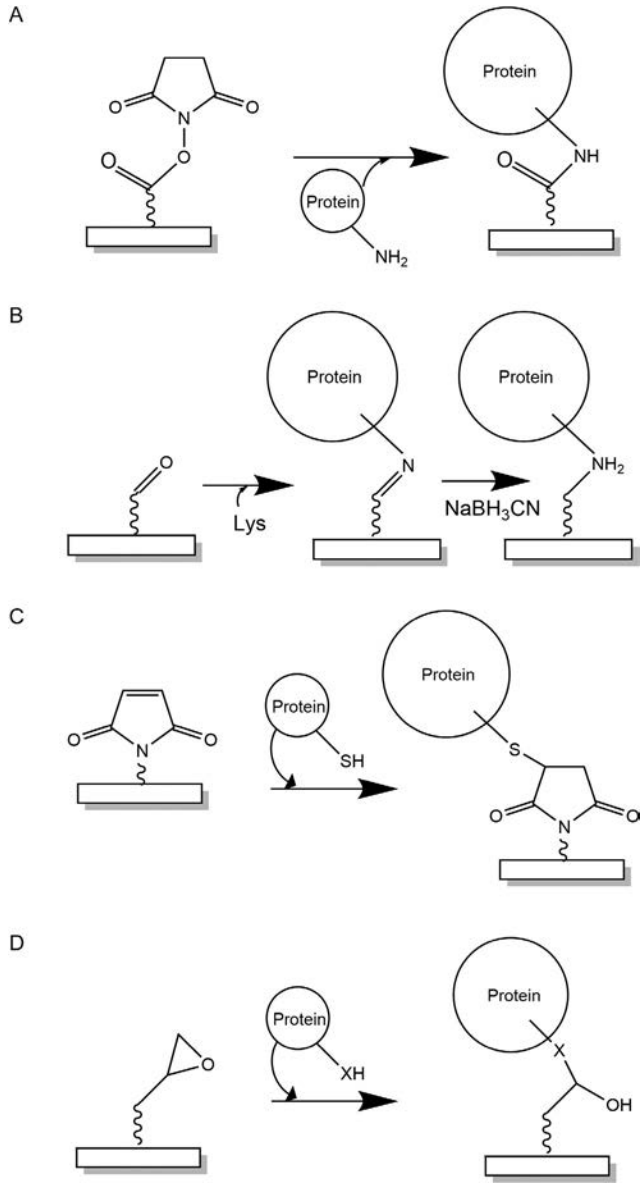

Fig. 6 Conventional covalent methods for immobilization with nucleophilic residues of proteins. Covalent bonds are formed through reaction with functional groups present on the protein surface. These methods can be used on unmodified proteins since they rely only on naturally present functional groups. (A) Reaction of lysine residues to NHS esters or aldehydes (B) and cysteine residue bonding to maleimide groups (C). Epoxides may react with either of the nucleophilic residues (D). *Adapted from Wong, L. S., Khan, F., & Micklefield, J. (2009). Selective covalent protein immobilization: Strategies and applications.* Chemical Reviews, 109*(9), 4025–4053. https://doi.org/10.1021/cr8004668.*

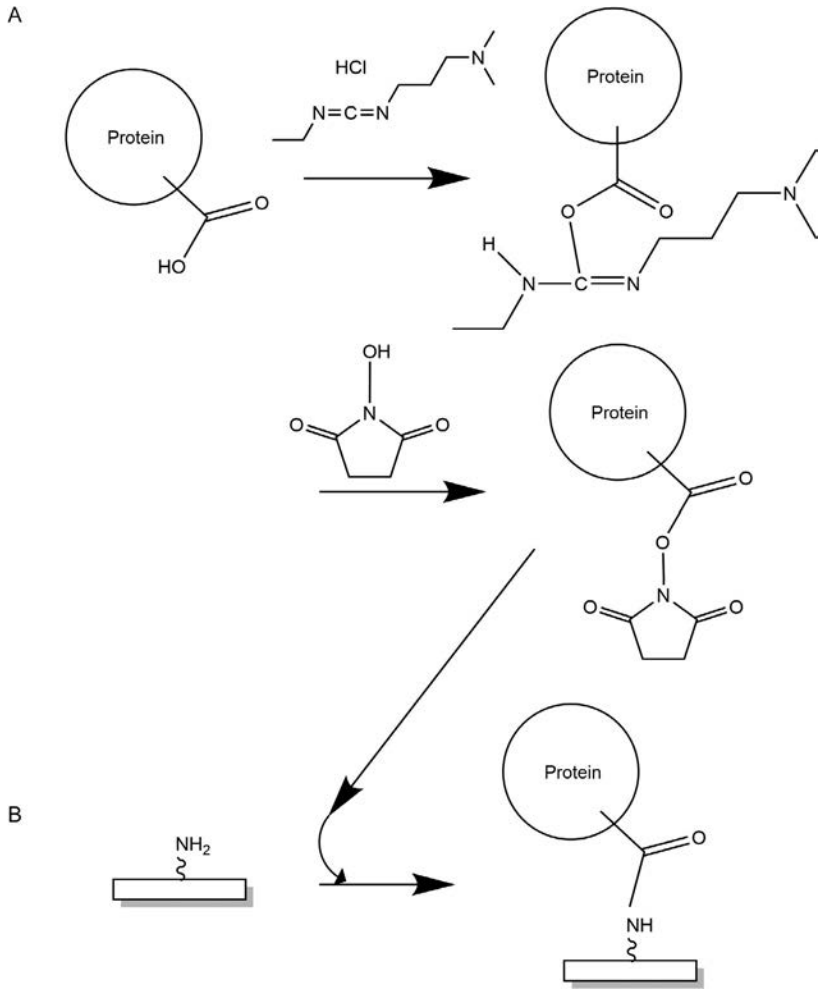

Fig. 7 Immobilization through acidic amino acid residues such as Glu and Asp. (A) By conversion to their corresponding active esters in situ with a carbodiimide coupling agent (EDC) 1-ethyl-3-(3-dimethylaminopropyl) carbodiimide followed by in situ generation of an NHS active ester (B) that is used to couple the protein.

come to the forefront (Briand et al., 2006; Ferretti, Paynter, Russell, Sapsford, & Richardson, 2000; Limbut, Kanatharana, Mattiasson, Asawatreratanakul, & Thavarungkul, 2006; Mauriz, Calle, Montoya, & Lechuga, 2006; Minamiki, Sasaki, Tokito, & Minami, 2017; Vaughan, O'Sullivan, & Guilbault, 1999). SAM is the generic name for techniques for generation of monomolecular layers of biological molecules on a variety

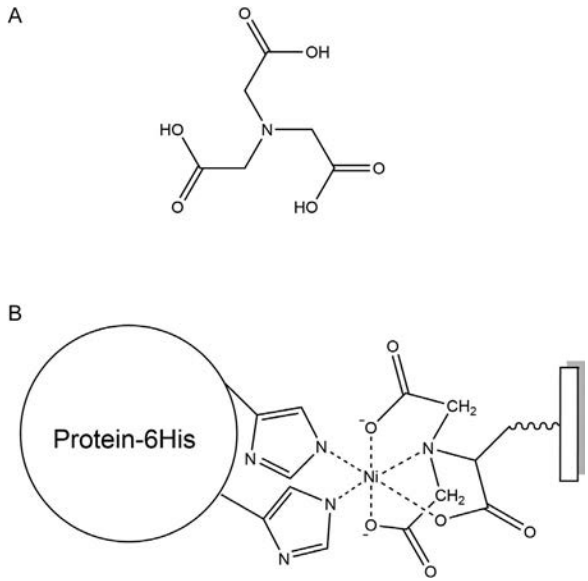

Fig. 8 Coupling via 6-histidine tagged proteins. (A) Nitrolotriacetic acid (NTA) used to functionalize the support. The chelating NTA moiety is first "activated" with the addition of a hexacoordinate metal ion (e.g., Ni^{2+}) followed by addition of the tagged protein. (B) The protein is immobilized on the support through chelation of the metal ion by the imidazole moieties of the His residues.

of substrates. Immobilization of proteins on SAMs allows reliable control over both the packing density and the environment of an immobilized protein at a substrate surface. In general, SAMs form by the spontaneous adsorption of amphiphilic adsorbates onto an appropriate substrate (Fig. 9) that is initially driven by chemical affinity between the adsorbates and the substrate. They can be formed either by gas phase deposition or from the liquid phase. They take advantage of the fact that many organic compounds have the capacity for self-assembly including long chain carboxylic acids or alcohols (RCOOH, ROH), where R is an alkyl chain, reacting with metal oxide substrates; organosilane species ($RSiX_3$, R_2SiX_2 or R_3SiX), where X is a chlorine atom or an alkoxy group, reacting with hydroxylated substrates (glass, silicon and aluminium oxide, etc.); and organosulfur-based species reacting with noble metal (gold, silver) surfaces. The latter is of great interest for biosensor construction due to their unique attractive features. Sulphur-containing compounds (alkanethiols, dialkyl disulfides and dialkyl sulfides) have a strong affinity for noble metal surfaces as they are spontaneously chemisorbed, with a regular organization and high thermal, mechanical

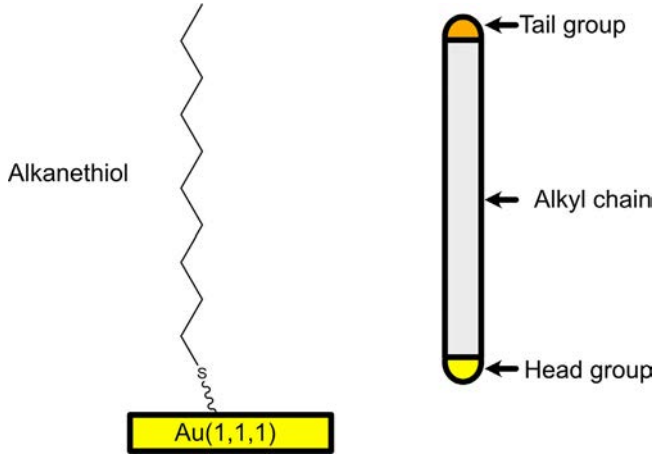

Fig. 9 Thiol-based SAMs. There are three important parts. The thiol moiety (head group) and chemisorption of this part to the substrate is the most important process in monolayer formation. An alkyl chain (methylene spacer) allows Van der Waals interaction between chains and provide a significant driving force for the adsorbate organization. The third part consists of a terminal functional group (tail group) to which a protein may be attached.

and chemical stability. These SAMs are easy to generate, they are densely packed and precisely oriented, and the thickness and the surface properties of the films can be easily adjusted. In thiol based SAMs the structure of the adsorbate molecule is divided into three parts (Fig. 9).

The first part is the thiol moiety (head group) and chemisorption of this part to the substrate is the most energetic and most important process in monolayer formation. The second part is an alkyl chain (methylene spacer), where Van der Waals interaction between chains provide a significant driving force for the adsorbate organization. The third part consists of a terminal functional group (tail group). In alkanethiol-based SAMs tail groups are methyl moieties that are exposed at the outermost surface of the monolayers and exert the most direct influence on the interfacial properties of the films. Because of their stability, orientation and ability to functionalize the terminal groups on the molecules, SAMs can offer a very convenient vehicle for covalent immobilization of biomolecules on gold surfaces for biosensor development. Often mixed SAMs formed by co-adsorption of mixtures of two thiols are used. One of these may be a thiol containing a functional group like a carboxylic acid that allows covalent attachment of a protein, the other being a diluting thiol without the functional group. This is used to reduce the surface concentration of functional groups, thus minimizing

steric hindrance, partial denaturation of the potential immobilized protein and nonspecific interactions that could produce interference signals. This can be very useful when immobilizing large proteins like antibodies but is less useful with small proteins such as OBPs.

3. Methods

3.1 Preparation of an OBP based sensor

This section describes immobilization of OBPs on quartz crystal microbalances (QCMs, Fig. 2) using a activated self-assembled monolayer of thioctic acid (TA) (Cali & Persaud, 2020; Persaud & Tuccori, 2014; Tuccori & Persaud, 2019). For this method the immobilized protein could be with or without a 6-Histidine tag.

3.2 Rationale

Thioctic acid (alpha-lipoic acid) is a molecule with a large disulfide-containing base, a short alkyl chain with four CH_2 units, and a carboxyl termination (Fig. 10). Carboxyl terminated SAMs of thioctic acid adsorbed on a gold surface evaporated on a quartz crystal are utilized for covalent immobilization of OBPs. Thioctic acid has distinct advantages for surface modification. The disulfide-containing base gives added stability and yields two gold-sulfur bonds per molecule in surface-attached species.

The widely utilized covalent protein immobilization method through amide bond formation is facilitated by reaction of amines on exposed lysine with N-hydroxysuccinimide (NHS) activated esters on the gold surface (Fig. 6). A carboxylic acid terminated self-assembled monolayer (SAM—in this case lipoic acid) is prepared by dipping the gold substrate (in this case QCM) into the thioctic acid. The SAM modified gold surface is then activated (functionalized) by reacting with 1-ethyl-3-[3-dimethylaminopropyl] carbodiimide hydrochloride (EDC). EDC reacts with a carboxyl group to form an active ester, an O-acylisourea. In general, covalent attachment of protein to the EDC reactive surface is possible. However, the EDC active surface is unstable to hydrolysis. To overcome this limitation, the use of N-hydroxysuccinimide (NHS) allows the conversion of the O-acylisourea intermediate into a relatively stable amine reactive NHS ester (Fig. 10). This NHS ester can then cross-link with amine groups on the protein through a covalent amide bond (Tan et al., 2011).

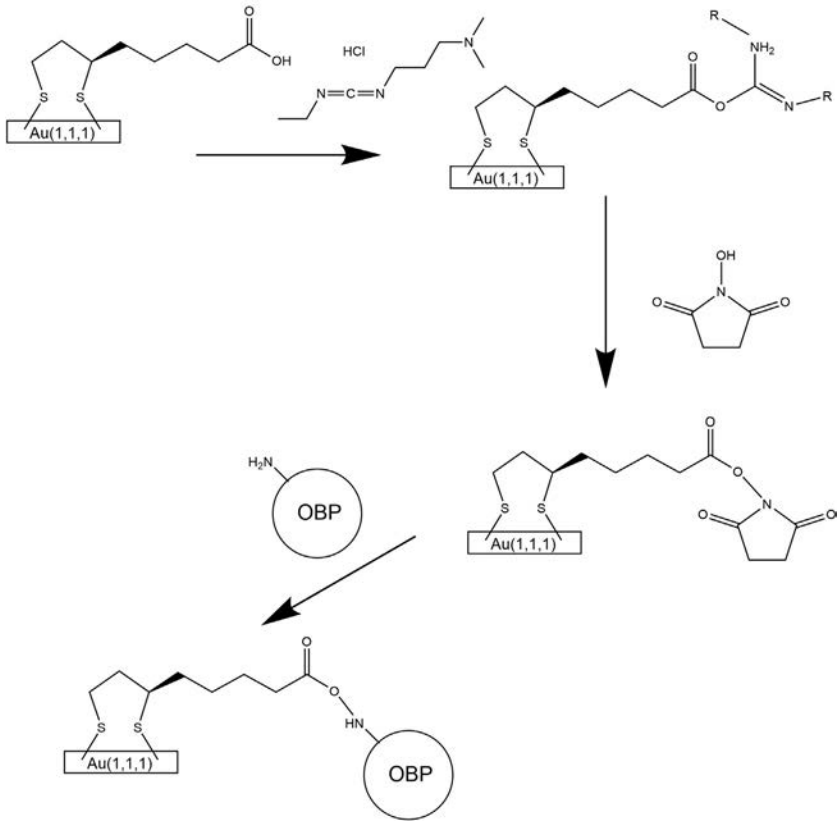

Fig. 10 Immobilization of OBPs on a gold surface using a SAM formed from thioctic acid. The SAM modified gold surface is activated by reacting with 1-ethyl-3-[3-dimethylaminopropyl] carbodiimide hydrochloride (EDC). EDC reacts with a carboxyl group to form an active ester, an O-acylisourea. N-hydroxysuccinimide (NHS) allows the conversion of the O-acylisourea intermediate into a relatively stable amine reactive NHS ester. This NHS ester can then cross-link with an amine group on the protein through a covalent amide bond.

3.3 Materials, equipment and reagents

Recombinant OBPs were produced in the laboratory standard procedures for the expression and purification of OBPs with or without a 6-Histidine tag (Cali & Persaud, 2020). All reagents used were of analytical grade purchased from Sigma-Aldrich, Fisher Scientific, or VWR. Genes were custom synthesized at Eurofins MWG GmbH, Ebensburg, Germany. The JLMQ USB interface for 4 QMB sensors (JLM Innovation GmbH, Tuebingen, Germany) was

used as a readout system for 20 MHz quartz crystal microbalances with gold coated electrodes that were fabricated by IMM-CNR, Italy. The SAW readout device was from Karlsruhe Institute of Technology (KIT), Germany. SAW transducers with the structure shown in Fig. 3B are utilized. Nanocrystalline diamond coated surface acoustic wave (SAW) sensors were produced using strategies reported by Manai et al. (2014) and Scorsone et al. (2016).

4. Protocols

4.1 Preparation of SAM onto QCMs

This procedure also applies to any gravimetric transducer that has a gold active surface.

This procedure should be carried out in a fume cupboard

1. Clean glass vials (of 2–4 mL capacity) by incubating with Piranha solution (1:3: 30% H_2O_2:H_2SO_4) for a few minutes. Remove the Piranha solution and rinse the vials with plenty of distilled water. Dry vials in an oven.
2. Place required number of QCMs into clean glass Petri dish. Add about 10 μL of Piranha solution to the gold surface of a QCM crystal. Leave it for a few minutes to remove any organic residues from the surface and to obtain hydrophilic gold surface. Make sure the Piranha solution does not touch the spring contacts at the edges of the crystal as these are made of steel and will corrode. Rinse the QCM with ddH_2O and let it dry at air. Repeat the whole procedure on the other side of the QCM. It is possible to remove the quartz resonators from the supports to carry out the procedure, but this can risk breaking the fragile quartz crystals.
3. To each cleaned vial add about 2 mL of a solution of 10 mM thioctic acid (TA) in ethanol, and then immerse one QCM into the vial. Then place the vials into a container with a loosely closed lid. Leave the reaction to continue for 20 h under slow nitrogen flow (20sccm/min). However, the procedure can be also be done without nitrogen flow in a dessicator under inert atmosphere. While the interaction of thioctic acid with gold is very rapid, the formation of a stable SAM takes many hours.
4. Rinse the QCMs with absolute ethanol to remove unbound molecules of TA and leave to dry in air. Place the QCMs into a clean Petri dish or glass vial for storage.

4.2 Activation of the SAM

This procedure is carried out on the lab bench

1. Place the Petri dish (es) containing the QCMs on your lab working bench. To activate the carboxylic acid groups of the TA SAM add 20 μL of a solution of 180 mM ethyl (dimethylaminopropyl) carbodiimide (EDC) and 180 mM of N-hydroxysuccinimide (NHS) in 10 mM sodium phosphate buffer (pH 7) to the gold surface of the QCM crystal. Close the Petri dish to stop the activation solution from evaporating. Leave the reaction to continue for 2 h at room temperature.
2. Rinse with ddH_2O and dry the crystal at air.
3. Repeat step 1 and 2 on the other side of the QCM.

4.3 Immobilization the OBP onto activated TA SAM

This procedure is carried out on the lab bench. Concentration of OBPs needed is between 0.5 and 1 mg/mL.

1. The immobilization of the proteins is performed by pipetting 10 μL of the OBP solution onto the gold surface containing the activated SAM and leaving it to react for an hour at room temperature.
2. Gently rinse with ddH_2O and then dry the crystal at air.
3. Repeat steps 1 and 2 on the other side of the QCM.

While some researchers block unreacted groups on the SAM using a solution of ethanolamine, it is simpler just to wash the surface with distilled water as the EDC/NHS activation is not stable.

5. Immobilization of OBPs on to nanocrystalline diamond coated transducers

5.1 Rationale

Diamond can be activated to produce hydrogen-terminated diamond surfaces and functionalized using the chemistry normally used for carbon. A suitable approach is use of hexanoic acid which is covalently attached to hydrogen-terminated diamond surfaces followed by ethyl(dimethylaminopropyl) carbodiimide (EDC)/N-hydroxysuccinimide (NHS) activation and coupling with OBPs. The first step of this method is the formation of hexanoic acid radical covalently onto the hydrogen-terminated diamond surface on SAW sensors. This covalent immobilization of aliphatic primary amines on hydrogen-terminated diamond is a nucleophilic substitution involving the formation of carbanion at the diamond surface in the presence of OH^- ions in solution.

The reaction of the protonated amine with the labile carbanion results in the release of ammonia and carbon-carbon covalent grafting of the aliphatic compound over the diamond surface.

5.2 Protocol

It is advisable to prepare replicate sensors for each protein. While the SAW devices are not as fragile as QCMs, care needs to be taken in handling them—use soft forceps such as those used for handling surface mount electronic devices and avoid touching the electrode surfaces.

1. Immerse the hydrogen-terminated diamond substrate SAW sensor into 2 mL of 1 mM solution of hexanoic acid (caproic acid-ACA) in 0.2 M phosphate buffer (pH 7.0) for 10 min.
2. Thoroughly rinse the sensor with ddH_2O and then dry under gentle N_2 flow.
3. Activate the carboxylic acid groups of the resulting SAM with a solution of 30 mM ethyl (dimethylaminopropyl) carbodiimide (EDC)/60 mM of N-hydroxysuccinimide (NHS) in 10 mM sodium phosphate buffer (pH 7) for 2 h at room temperature.
4. Rinse with ddH_2O and dry the sensor at air.
5. Expose the activated diamond substrate to a small quantity of OBP solution (0.5–1 mg/mL in 50 mM $NaHCO_3$ buffer, pH 8.0) for 2 h.
6. Rinse the sensor thoroughly with ddH_2O and store in phosphate buffer saline (PBS) solution at 4 °C or dry in air and store in a vial at 4 °C.

6. Immobilization of histidine tagged OBPs

6.1 Rationale

The purpose of this method is to control the orientation of the proteins immobilized on the surface Here NTA forms a chemical linker between the diamond surface and the protein. This approach involves formation of NTA SAM onto diamond surface. NTA has the ability to bind nickel (II), and the resulting NTA-Ni^{2+} complex has a higher affinity to histidine thus enabling the immobilization of 6-Histidine tagged OBPs (Fig. 8).

6.2 Protocol

1. Immerse the hydrogen-terminated diamond substrate SAW sensor in a solution of 1 mM of Nα, Nα-Bis-(carboxy-methyl)-L-lysine hydrate (≥97%) (NTA) in 0.2 M phosphate buffer, pH 7.0, for 10 min.
2. Thoroughly rinse the sensor with ddH_2O and then dry under gentle N_2 flow.

3. To activate the NTA SAM, immerse the diamond surface in nickel (II) chloride hexahydrate (99.99%) solution for 2 h at room temperature.
4. Immerse the NTA-Ni2+ complex terminated diamond surfaces in the 6-Histidine tagged OBP solution (1 mg/mL in 50 mM phosphate buffer saline (PBS), pH 8.0) for 2 h.
5. Rinse the sensor thoroughly with ddH_2O and store in phosphate buffer saline (PBS) solution.

7. Analyte vapor generation

OBP based gas sensors can respond to different analytes from ppb to ppm levels and test apparatus used very much depends on the nature of the analyte of interest, the saturated vapor pressure and the whether complex mixtures or single components are used. Burlachenko et al. review appropriate sampling methods for electronic noses (Burlachenko, Kruglenko, Snopok, & Persaud, 2016).

For simple systems an automated flow system consisting of electronically controlled solenoid valves and mass flow controllers is used to produce and deliver selected concentrations of solvent vapors to the detectors. To obtain the desired analyte concentration, a stream of carrier gas is passed through a bubbler that is filled with an analyte or solvent of interest. Saturation of the carrier gas with the solvent vapor can be verified through measurement of the rate of mass loss of the solvent in the bubbler. The vapor-saturated carrier gas is then diluted with pure carrier gas (which in this case can be normal room air, or air from a cylinder that has added humidity) through the use of mass flow controllers.

For simple tests—generation of a saturated vapor headspace can suffice for testing operation of the OBP sensor, especially when dealing with substances of low volatility. The substance can be placed in closed 40 mL vial. Prepare each analyte sample at least in replicate. As an example, between 1 and 20 μL of the liquid analytes (e.g., acetone) or 1–30 mg of the solid analytes (e.g., tobacco) into closed 40 mL vials (Fig. 11) and left for 1 h (for highly volatile compounds) to few hours (for less volatile compounds) at room temperature to allow the formation of the saturated vapors.

To generate very low concentrations of vapors permeation tubes may be used. They provide a stable concentration of a specific trace chemical, including those with low vapor pressures. When held at a constant temperature, these devices emit a small stable flow of chemical vapor that is measured in nanograms or nanoliters per minute (Mitchell, 2000).

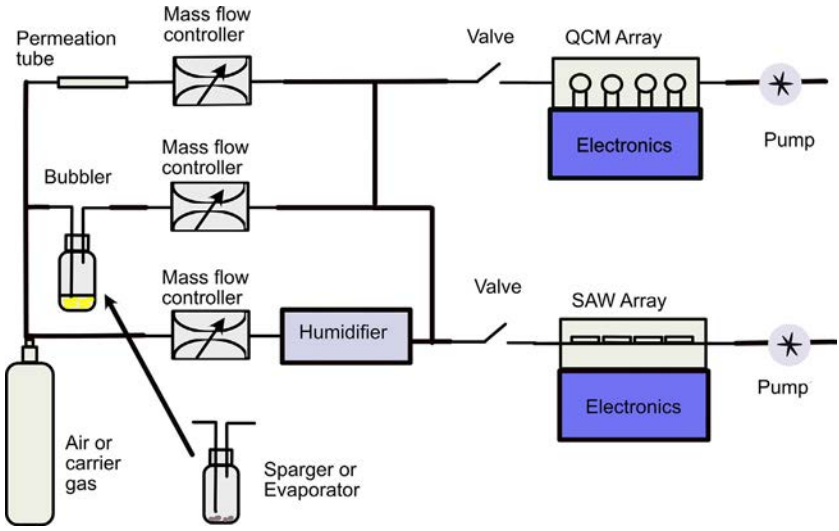

Fig. 11 Gas Rig for testing OBP sensors using either QMB or SAW platforms. Analyte generation may be through bubblers, permeation tubes, spargers, headspace stripping devices or others. The generated vapor is diluted with clean humidified air via mass flow controllers to produce desired concentration ranges of vapors to be applied to the sensors. A small pump aspirates vapor across the sensor arrays.

7.1 Testing of sensors with analyte vapors

This procedure is carried out in the fume cupboard. The QCM measurements are carried out at 22% RH or above in air at room temperature. Extremely low relative humidity should be avoided as the protein requires a shell of water molecules to retain the active tertiary structure and active binding pocket.

1. Device set up: Mount (insert) the QCM biosensors developed above into the QCM reader sensing chamber. Then place the device into a fume cupboard. Connect the device to the computer and a pump (unless the device has an embedded pump). The device should have inlet and outlet tubing connectors. Different QCM readers have different numbers of sensors that they can accommodate. The JLMQ device can hold up to 4 sensors while others can accommodate up to 12 sensors. For newly made biosensors, it is highly recommended to allow them to stabilize by passing clean air over the sensors for several hours. An example set up is shown in Fig. 11.
2. Device operation: Start the software in use and the pump to pass clean air (approximately 0.1 L/min—flow rate depends on the sampling system utilized) through to the sensors to allow the establishment of the baseline. Small rotary or diaphragm pumps for gases are available from a range of suppliers.

3. Detection of the vapor from target analytes: Any tubing used should be inert to minimize adsorption/absorption of analyte vapor. Suitable materials are polytetrafluoroethylene (PTFE) or perfluoroalkoxy (PFA). For the flow rates normally used, tubing can be 3.2 or 4 mm diameter dependent on connectors that are used. The sample vial containing the analyte saturated vapor should have tubing that will be connected to the measurement device via a connector. The pump will pull the analyte sample through to the device sensing chamber. Allow the exposure of the analyte vapor to the sensors for around 10–20 s (but this is up to the operator to decide according to the quality of the signal obtained). Save/export the results according to the appropriate data format (e.g., text file, CSV file, Excel file, etc.).

8. Safety considerations and standards

Piranha solution is highly corrosive and adequate person protection should be implemented.

When using gases and volatile analytes a fume hood with adequate ventilation should be used.

9. Analysis

Fig. 12 shows the raw data recorded from an OBP-QMB sensor to a saturated headspace of cocaine hydrochloride. This has an extremely low vapor pressure (SVP 1.84211×10^{-11} atm at 20 °C), but the device produces a small but useful signal, illustrating the potential sensitivity of such devices. A decrease in frequency is observed due to the increased mass loading of the QMB and this returns to normal frequency as the analyte desorbs from the sensor.

Fig. 13 shows raw data recorded from an array of eight SAW-OBP sensors (S1–S8) with immobilized OBPs from a range of insect and mammalian OBPs. Like QMBs the actual change in frequency is a decrease, but by convention the data have been normalized with respect to sign and are shown as positive changes in frequency. Responses are shown to pulses of (A) alpha-pinene vapor and (B) tobacco vapor. The frequency changes above are much higher than those observed with QMBs due to the higher operating frequency of the devices (433 MHz for SAW devices as opposed to 20 MHz for QMBs). It is seen that different OBPs in the array respond very differently to the different samples presented to them. Using such an array allows traditional "electronic nose" approaches to be used to discriminate different classes of volatile chemicals or indeed complex mixtures of volatile compounds.

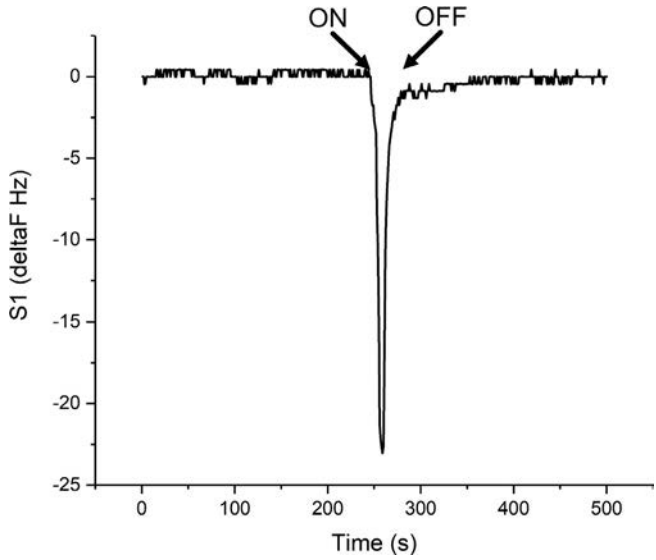

Fig. 12 Raw data response of an OBP-QMB sensor to cocaine-HCl vapor. A saturated vapor headspace was aspirated across the sensor array and the frequency change of each sensor was recorded. A decrease in frequency is observed as the mass of the QMB increased due to the loading of the adsorbed analyte, and this is reversible when clean air is applied to the sensor.

The appropriate data processing methods for gas sensor arrays are reviewed in detail by Persaud (2013). Pattern recognition in an "electronic nose" system may be regarded as a branch of artificial intelligence that involves the mimicking of human intelligence to solve chemical problems. Two main approaches to pattern recognition are commonly used: parametric and non-parametric. Parametric methods rely upon obtaining or estimating the probability density function of the parameters used to characterize the response of a system. Conversely, non-parametric methods require no assumption about the fundamental statistical distributions of data. Two types of non-parametric learning or classification methods are available: supervised and non-supervised (De Vito, Fattoruso, Pardo, Tortorella, & Di Francia, 2012; Hines, Llobet, & Gardner, 1999; Pardo & Sberveglieri, 2005). Supervised methods involve the learning of data based on advance knowledge of the classification, whereas unsupervised methods make no prior assumption about the sample classes but try to separate groups or clusters. This is a large and complex field that is evolving very rapidly with developments in advanced algorithms as well as dedicated integrated circuits capable of encoding neural networks.

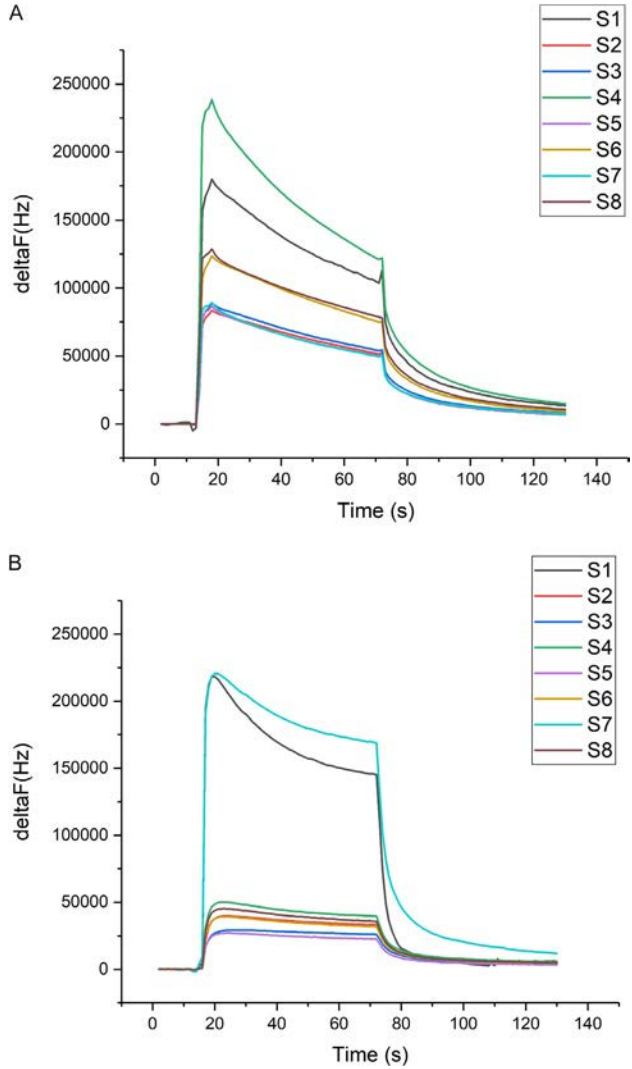

Fig. 13 Responses of an OBP-SAW array comprising eight OBPs from insect and mammalian origin. S1–S8 are individual SAW devices with different immobilized proteins (A) responses to a saturated vapor of alpha-pinene (B) responses to tobacco headspace vapor. The responses of individual OBPs are very different dependent of the analyte components reflecting the diversity of interactions that may be possible. The generated pattern of responses can be used to discriminate a range of different volatile chemicals or complex mixtures such as tobacco.

10. Related techniques

Apart from self-assembled monolayers, another major technique for the fabrication of supramolecular structures on surfaces is the Langmuir-Blodgett (LB) method. Langmuir films are composed of an organized monolayer of amphiphilic molecules at a liquid/gas interface. These molecules, by virtue of possessing a hydrophobic tail and a hydrophilic head, are spontaneously oriented at a liquid/gas interface. In LB amphiphilic molecules and macromolecules with amphiphilic segments are transferred onto a solid support by vertically lifting the support through the film.

SAMs can either be formed directly from solution (as reported here) or by gas phase deposition (Shuturminska, O'Malley, Collis, Conde, & Azevedo, 2018). While gold is the preferred noble substrate for SAM formation for protein immobilization, other metals have been used including copper, iron and silver. Copper is a widely used due to its electric conduction and thermal properties. Iron has been investigated due to its magnetic hyperthermia properties. The geometry and lattice structure of the metal surface can be utilized further by evenly distributing specific ligands (such as aromatic peptides and imidazoles with alkyl tails) over the surface to enhance and stabilize the metal properties. Silicate glass is also being used since unlike a metal surface; it is relatively chemically inert due to the strength of Si—O bond in the silica network. Glass surfaces need to be modified by etching (using extreme pH to break Si—O bonds) to form free hydroxyl groups on the surface which provide linkage points where other molecules can be chemically grafted. Alternatives to silicates and metals for SAMs are the carbon-based substrates known as nanocarbons. Examples of these nanocarbons include fullerenes, carbon nanotubes (CNTs) and graphene. Apart from SAMs with terminal carboxylic acid and SAMs with terminal NTA, other SAMs used for protein immobilization include SAMs with terminal amino groups (glutaraldehyde reaction to link with an amino group of the objective substance), SAMs with terminal biotin (biotin immobilization combined with streptavidin labeled objective substance), and SAMs with latent aldehyde (Hahn et al., 2007).

The formation of SAMs is not restricted to single types of molecules, and so mixed SAMs are also used. There are two ways to prepare mixed SAMs. One is to prepare by mixing two different solutions of alkane thiol derivatives, and the other is to use an asymmetric disulfide derivatives. Nonspecific adsorption caused by electrostatic interaction is not un-common in single SAM, but occurrence of nonspecific adsorption can be prevented

significantly by using mixed SAM, particularly when dealing with large proteins. One example of mixed SAM used for biosensor applications is the use of alkane thiol derivative introduced oligoethyleneglycol moiety (Kyo, Usui-Aoki, & Koga, 2005; Laibinis, Fox, Folkers, & Whitesides, 1991).

Other methods of immobilization of OBPs to form sensors have also been reported. These range from simple drop casting of OBPs on to SAW transducers (Di Pietrantonio et al., 2015) to the use of laser-induced forward transfer (LIFT) (Duocastella, Colina, Fernández-Pradas, Serra, & Morenza, 2007) by the same authors for depositing OBPs on to SAW transducers.

11. Pros and cons

Pros	Cons
One of the important features of SAM is simple preparation as no special equipment is required to prepare SAM layers. After chemisorption, the SAMs are stable in ambient temperature and pressure for prolonged periods of time that allows subsequent chemical functionalization of the assembled molecules with biological entities such as proteins. The stability of SAMs during chemical functionalization further expands their applications, such as in microelectronics.	Even though the preparation of SAMs from solution is relatively easy, care needs to be taken to ensure their formation is optimal under certain conditions. E.g., Selection of appropriate solvents—although most polar solvents including dimethylformamide (DMF), dichloromethane (DCM), and acetone can assist the formation of SAMS, preparation of SAMs of alkyl thiols is typically carried out in pure ethanol which is optimal to guarantee production of defect-free SAMs.
QCM and SAW sensors can measure intermolecular interaction without labeling measuring objects by monitoring the changes of frequencies of the sensors. Once immobilized on QCMs and SAWs OBP biosensors remains stable and be able to continue to sensitively detect the target analytes vapor up to 1 year. Having affinity to a great number of organic molecules (odorants and pheromones) makes OBPs attractive to build reliable biosensors for different applications.	There could be small daily variations in response due to variations in the concentrations of saturated vapor generated at ambient temperatures. Having affinity to a great number of organic molecules makes OBP biosensors susceptible to cross-sensitivity to a range of substances. Hence, they are best implemented as arrays of sensors containing different OBPs with different binding affinities to a range of vapors.

Continued

—cont'd

Pros	Cons
OBPs have binding pockets capable of binding certain groups of chemicals with high specificity.	Binding pockets are not completely selective so cross-sensitivity will be observed across a range of analytes. Nonspecific binding is also possible on the outside of the proteins as well as on the supports used to immobilize the proteins.

12. Troubleshooting and optimization

Problem	Solution
OBP biosensors are sensitive to the humidity of the environment. If too dry they will stop working completely.	Never expose the OBP biosensors to completely dry gases. If that happens for any reason exposure to water vapor often leads to complete recovery. It is recommended to expose the sensors to a pulse of water vapor on a regular basis.
Occasionally OBP sensors may lose activity suddenly—especially if exposed to high concentrations of certain vapors.	If the sensor does lose activity suddenly exposure to water vapor often leads to recovery.

13. Summary

Methods are described enabling recombinant OBPs with or without a 6-Histidine tag to be immobilized using self-assembled monolayers on gravimetric transducers to create functional sensors capable of sensing a range of volatile organic compounds with selectivity dependent on the binding pockets of the OBPs. SAMs allow well oriented covalent attachment of proteins on to transducers surfaces. NTA immobilization utilizing 6-histidine tags attached on to the N-terminal or the C-terminal of the OBPs can produce well ordered stable films without affecting access of ligands to the protein binding sites.

Acknowledgments

Khasim Cali was supported though the CURSOR project which has received funding from the European Union's Horizon 2020 research and innovation programme under grant agreement No 832790 and from the Japan Science and Technology Agency.

Elena Tuccori was supported through a Marie Curie Early Stage Researcher grant (FLEXSMELL grant agreement No 2009-238454).

The opinions expressed in this document reflect only the author's view and reflects in no way the European Commission's opinions. The European Commission is not responsible for any use that may be made of the information it contains.

References

Briand, E., Salmain, M., Herry, J. M., Perrot, H., Compère, C., & Pradier, C. M. (2006). Building of an immunosensor: How can the composition and structure of the thiol attachment layer affect the immunosensor efficiency? *Biosensors and Bioelectronics*, *22*(3), 440–448. https://doi.org/10.1016/j.bios.2006.05.018.

Burlachenko, J., Kruglenko, I., Snopok, B., & Persaud, K. (2016). Sample handling for electronic nose technology: State of the art and future trends. *TrAC Trends in Analytical Chemistry*, *82*, 222–236. https://doi.org/10.1016/j.trac.2016.06.007.

Cady, W. G. (1921). The piezo-electric resonator. *Proceedings Institute of Radio Engineers*, *6*, 83–114.

Cady, W. G. (1946). *Piezoelectricity* (1st ed.). New York and London: McGraw-Hill.

Cali, K., & Persaud, K. C. (2020). Modification of an Anopheles gambiae odorant binding protein to create an array of chemical sensors for detection of drugs. *Scientific Reports*, *10*(1), 1–13. https://doi.org/10.1038/s41598-020-60824-7.

Cali, K., Scorsone, E., & Persaud, K. C. (2019). Odour sensing using arrays of odorant binding proteins. In *Chemical senses, Vol. 44* (p. E49). Oxford, England: Oxford University Press.

Chang, Y., Tang, N., Qu, H., Liu, J., Zhang, D., Zhang, H., et al. (2016). Detection of volatile organic compounds by self-assembled monolayer coated sensor array with concentration-independent fingerprints. *Scientific Reports*, *6*, 1–12. https://doi.org/10.1038/srep23970.

Chevallier, E., Scorsone, E., & Bergonzo, P. (2009). Modified diamond nanoparticles as sensitive coatings for chemical SAW sensors. *Procedia Chemistry*, *1*(1), 943–946. https://doi.org/10.1016/j.proche.2009.07.235.

Curie, J., & Curie, P. (1880). Comptes rendus des séances de l'Académie des Sciences. *Journal of Chemical Information and Modeling*, 1–30. https://doi.org/10.1017/CBO9781107415324.004.

De Vito, S., Fattoruso, G., Pardo, M., Tortorella, F., & Di Francia, G. (2012). Semi-supervised learning techniques in artificial olfaction: A novel approach to classification problems and drift counteraction. *IEEE Sensors Journal*, *12*, 3215–3224. https://doi.org/10.1109/JSEN.2012.2192425.

Di Natale, C., Martinelli, E., Paolesse, R., D'Amico, A., Filippini, D., & Lundström, I. (2008). An experimental biomimetic platform for artificial olfaction. *PLoS One*, *3*(9), e3139. https://doi.org/10.1371/journal.pone.0003139.

Di Pietrantonio, F., Benetti, M., Cannatà, D., Verona, E., Palla-Papavlu, A., Fernández-Pradas, J. M., et al. (2015). A surface acoustic wave bio-electronic nose for detection of volatile odorant molecules. *Biosensors and Bioelectronics*, *67*(October 2016), 516–523. https://doi.org/10.1016/j.bios.2014.09.027.

Duocastella, M., Colina, M., Fernández-Pradas, J. M., Serra, P., & Morenza, J. L. (2007). Study of the laser-induced forward transfer of liquids for laser bioprinting. *Applied Surface Science*, *253*(19), 7855–7859. https://doi.org/10.1016/j.apsusc.2007.02.097.

Fanget, S., Hentz, S., Puget, P., Arcamone, J., Matheron, M., Colinet, E., et al. (2011). Gas sensors based on gravimetric detection—A review. *Sensors and Actuators, B: Chemical*, *160*(1), 804–821. https://doi.org/10.1016/j.snb.2011.08.066.

Ferretti, S., Paynter, S., Russell, D. A., Sapsford, K. E., & Richardson, D. J. (2000). Self-assembled monolayers: A versatile tool for the formulation of bio- surfaces. *TrAC Trends in Analytical Chemistry*, *19*, 530–540. https://doi.org/10.1016/S0165-9936(00)00032-7.

Go, D. B., Atashbar, M. Z., Ramshani, Z., & Chang, H. C. (2017). Surface acoustic wave devices for chemical sensing and microfluidics: A review and perspective. *Analytical Methods Royal Society of Chemistry*, *9*, 4112–4134. https://doi.org/10.1039/c7ay00690j.

Hahn, C. D., Leitner, C., Weinbrenner, T., Schlapak, R., Tinazli, A., Tampé, R., et al. (2007). Self-assembled monolayers with latent aldehydes for protein immobilization. *Bioconjugate Chemistry*, *18*(1), 247–253. https://doi.org/10.1021/bc060292e.

Hines, E. L., Llobet, E., & Gardner, J. W. (1999). Electronic noses: A review of signal processing techniques. *IEE Proceedings—Circuits, Devices and Systems*, 146(6), 297. https://doi.org/10.1049/ip-cds:19990670.

Hochuli, E., Bannwarth, W., Dobeli, H., Gentz, R., & Stuber, D. (1988). Genric approach to facilitate purification of recombinant proteins with a novel metal chelate adsorbent. *Nature Biotechnology*, *6*, 1321–1325. (November). https://doi.org/10.1038/nbt1188-1321.

Katzir, S. (2012). Who knew piezoelectricity? Rutherford and Langevin on submarine detection and the invention of sonar. *Notes and Records of the Royal Society Royal Society*, *66*(2), 141–157. https://doi.org/10.1098/rsnr.2011.0049.

King, W. H., Jr. (1972). The use of resonating devices to make small mass measurements. *Bulletin of the New York Academy of Medicine*, *48*(2), 459–464.

Kyo, M., Usui-Aoki, K., & Koga, H. (2005). Label-free detection of proteins in crude cell lysate with antibody arrays by a surface plasmon resonance imaging technique. *Analytical Chemistry*, 77(22), 7115–7121. https://doi.org/10.1021/ac050884a.

Lack, F. R., Willard, G. W., & Fair, I. E. (1930). Some improvements in quartz crystal circuit elements. *Bell System Technical Journal*, *453*(1), 453–463.

Laibinis, P. E., Fox, M. A., Folkers, J. P., & Whitesides, G. M. (1991). Comparisons of self-assembled monolayers on silver and gold: Mixed monolayers derived from HS(CH2) 21X and HS(CH2)10Y (X, Y = CH3, CH2OH) have similar properties. *Langmuir*, *7*(12), 3167–3173.

Lamb, H. (1917). On waves in an elastic plate. *Proceedings of the Royal Society of London, Series A*, *93*(648), 114–128. https://doi.org/10.1098/rspa.1917.0008.

Länge, K., Rapp, B. E., & Rapp, M. (2008). Surface acoustic wave biosensors: A review. *Analytical and Bioanalytical Chemistry*, *391*(5), 1509–1519. https://doi.org/10.1007/s00216-008-1911-5.

Limbut, W., Kanatharana, P., Mattiasson, B., Asawatreratanakul, P., & Thavarungkul, P. (2006). A comparative study of capacitive immunosensors based on self-assembled monolayers formed from thiourea, thioctic acid, and 3-mercaptopropionic acid. *Biosensors and Bioelectronics*, *22*(2), 233–240. https://doi.org/10.1016/j.bios.2005.12.025.

Lippmann, M. G. (1881). On the principle of the conservation of electricity. *The London, Edinburgh, and Dublin Philosophical Magazine and Journal of Science*, *12*, 151–154. https://doi.org/10.1080/14786448108627081.

Love, A. E. H. (1911). *Some problems of geodynamics*. Cambridge: University Press.

Manai, R., Scorsone, E., Rousseau, L., Ghassemi, F., Possas Abreu, M., Lissorgues, G., et al. (2014). Grafting odorant binding proteins on diamond bio-MEMS. *Biosensors and Bioelectronics*, *60*, 311–317. https://doi.org/10.1016/j.bios.2014.04.020.

Mastromatteo, U., & Villa, F. F. (2013). High sensitivity acoustic wave AlN/Si mass detectors arrays for artificial olfactory and biosensing applications: A review. *Sensors and Actuators B: Chemical*, *179*, 319–327. https://doi.org/10.1016/j.snb.2012.10.033.

Mauriz, E., Calle, A., Montoya, A., & Lechuga, L. M. (2006). Determination of environmental organic pollutants with a portable optical immunosensor. *Talanta*, *69*(2), 359–364. https://doi.org/10.1016/j.talanta.2005.09.049.

Minamiki, T., Sasaki, Y., Tokito, S., & Minami, T. (2017). Label-free direct electrical detection of a histidine-rich protein with sub-femtomolar sensitivity using an organic field-effect transistor. *ChemistryOpen*, *6*(4), 472–475. https://doi.org/10.1002/open.201700070.

Mitchell, G. D. (2000). A review of permeation tubes and permeators. *Separation and Purification Methods*, *29*(**1**), 119–128. Taylor & Francis Group. https://doi.org/10.1081/SPM-100100005.

Muñoz-Aguirre, S., Nakamoto, T., & Moriizumi, T. (2005). Study of deposition of gas sensing films on quartz crystal microbalance using an ultrasonic atomizer. *Sensors and Actuators B: Chemical*, *105*(2), 144–149. https://doi.org/10.1016/j.snb.2004.05.063.

Nakamoto, T., Fukunishi, K., & Moriizumi, T. (1990). Identification capability of odor sensor using quartz-resonator array and neural-network pattern recognition. *Sensors and Actuators B: Chemical*, *1*(1–6), 473–476. https://doi.org/10.1016/0925-4005(90)80252-U.

Nazemi, H., Joseph, A., Park, J., & Emadi, A. (2019). Advanced micro-and nano-gas sensor technology: A review. *Sensors (Switzerland)*, *19*(6), 1285. https://doi.org/10.3390/s19061285.

Pardo, M., & Sberveglieri, G. (2005). Classification of electronic nose data with support vector machines. *Sensors and Actuators, B: Chemical*, *107*(2), 730–737. https://doi.org/10.1016/j.snb.2004.12.005.

Persaud, K. C. (2013). Engineering aspects of olfaction. In *Neuromorphic olfaction* (pp. 1–58). Dordrecht: Springer. https://doi.org/NBK298822 [bookaccession].

Persaud, K. C., & Tuccori, E. (2014). Biosensors based on odorant binding proteins. Vol. 9789401786133, Bioelectronic nose: Integration of biotechnology and nanotechnology (pp. 171–190). Netherlands: Springer. https://doi.org/10.1007/978-94-017-8613-3_10.

Pierce, G. W. (1923). Piezoelectric crystal resonators and crystal oscillators applied to the precision calibration of wavemeters. *Proceedings of the American Academy of Arts and Sciences*, *59*(4), 81. https://doi.org/10.2307/20026061.

Possas-Abreu, M., Ghassemi, F., Rousseau, L., Scorsone, E., Descours, E., & Lissorgues, G. (2017). Development of diamond and silicon MEMS sensor arrays with integrated readout for vapor detection. *Sensors (Basel, Switzerland)*, *17*(6), 1163. https://doi.org/10.3390/s17061163.

Possas-Abreu, M., Rousseau, L., Ghassemi, F., Lissorgues, G., Habchi, M., Scorsone, E., et al. (2017). Biomimetic diamond MEMS sensors based on odorant-binding proteins: Sensors validation through an autonomous electronic system. In *ISOEN 2017—ISOCS/IEEE international symposium on olfaction and electronic nose, proceedings*. https://doi.org/10.1109/ISOEN.2017.7968909.

Rayleigh, L. (1885). On waves propagated along the plane surface of an elastic solid. *Proceedings of the London Mathematical Society*, *s1–17*(1), 4–11.

Sauerbrey, G. (1959). Verwendung von Schwingquarzen zur Wägung dünner Schichten und zur Mikrowägung. *Zeitschrift für Physik*, *155*, 206–222. https://doi.org/10.1007/BF01337937.

Scorsone, E., Manai, R., Ricatti, M. J., Redaelli, M., Bergonzo, P., Persaud, K. C., et al. (2016). Major urinary proteins on nanodiamond-based resonators toward artificial olfaction. *IEEE Sensors Journal*, *16*(17), 6543–6550. https://doi.org/10.1109/JSEN.2016.2585187.

Shuturminska, K., O'Malley, C., Collis, D. W. P., Conde, J., & Azevedo, H. S. (2018). Displaying biofunctionality on materials through templated self-assembly. In *Self-assembling biomaterials: Molecular design, characterization and application in biology and medicine* (pp. 341–370). Elsevier. https://doi.org/10.1016/B978-0-08-102015-9.00018-6.

Tan, Y. H., Schallom, J. R., Ganesh, N. V., Fujikawa, K., Demchenko, A. V., & Stine, K. J. (2011). Characterization of protein immobilization on nanoporous gold using atomic force microscopy and scanning electron microscopy. *Nanoscale*, *3*(8), 3395–3407. https://doi.org/10.1039/c1nr10427f.

Thundat, T., Oden, P. I., & Warmack, R. J. (1997). Microcantilever sensors. *Microscale Thermophysical Engineering*, *1*(3), 185–199. https://doi.org/10.1080/108939597200214.

Tuccori, E., & Persaud, K. C. (2019). Pheromone detection using odorant binding protein sensors. In *ISOEN 2019—18th international symposium on olfaction and electronic nose, proceedings*. https://doi.org/10.1109/ISOEN.2019.8823345.

Tukkiniemi, K., Rantala, A., Nirschl, M., Pitzer, D., Huber, T., & Schreiter, M. (2009). Fully integrated FBAR sensor matrix for mass detection. In *Vol. 1. Procedia chemistry* (pp. 1051–1054). Elsevier. https://doi.org/10.1016/j.proche.2009.07.262.

Vaughan, R. D., O'Sullivan, C. K., & Guilbault, G. G. (1999). Sulfur based self-assembled monolayers (SAM's) on piezoelectric crystals for immunosensor development. *Fresenius' Journal of Analytical Chemistry*, *364*(1), 54–57. https://doi.org/10.1007/s002160051300.

Vogt, B. D., Lin, E. K., Wu, W.-L., & White, C. C. (2004). Effect of film thickness on the validity of the Sauerbrey equation for hydrated polyelectrolyte films. *The Journal of Physical Chemistry B*, *108*, 12685–12690. https://doi.org/10.1021/jp0481005.

Voiculescu, I., & Nordin, A. N. (2012). Acoustic wave based MEMS devices for biosensing applications. *Biosensors and Bioelectronics*, *33*(1), 1–9. https://doi.org/10.1016/j.bios.2011.12.041.

Weiss, P. (1906). La variation du ferromagnetisme du temperature. *Comptes Rendus*, *143*, 1136–1149.

White, R. M., & Voltmer, F. W. (1965). Direct piezoelectric coupling to surface elastic waves. *Applied Physics Letters*, 7(12), 314–316. https://doi.org/10.1063/1.1754276.

Wong, L. S., Khan, F., & Micklefield, J. (2009). Selective covalent protein immobilization: Strategies and applications. *Chemical Reviews*, *109*(9), 4025–4053. https://doi.org/10.1021/cr8004668.

Zhang, M., Du, L., Fang, Z., & Zhao, Z. (2017). A sensitivity-enhanced film bulk acoustic resonator gas sensor with an oscillator circuit and its detection application. *Micromachines*, *8*(1), 25. https://doi.org/10.3390/mi8010025.

Zhang, Y., Luo, J., Flewitt, A. J., Cai, Z., & Zhao, X. (2018). Film bulk acoustic resonators (FBARs) as biosensors: A review. *Biosensors and Bioelectronics*, *116*, 1–15. https://doi.org/10.1016/j.bios.2018.05.028.

Further reading

Pinnaduwage, L. A., Hawk, J. E., Boiadjiev, V., Yi, D., & Thundat, T. (2003). Use of microcantilevers for the monitoring of molecular binding to self-assembled monolayers. *Langmuir*, *19*, 7841–7844. https://doi.org/10.1021/LA034969N.